

MASS, METALLICITY AND MORPHO-KINEMATICS IN COSMOLOGICAL SIMULATIONS

Zenocratti L. J.¹, De Rossi M. E.^{2,3}, Lara-López M. A.⁴, Theuns T.⁵

(1) Facultad de Ciencias Astronómicas y Geofísicas, Universidad Nacional de La Plata, Paseo del Bosque s/n, B1900FWA, La Plata, Argentina
(2) Universidad de Buenos Aires, Facultad de Ciencias Exactas y Naturales y Ciclo Básico Común. Buenos Aires, Argentina
(3) CONICET-Universidad de Buenos Aires, Instituto de Astronomía y Física del Espacio (IAFE), Buenos Aires, Argentina
(4) DARK, Niels Bohr Institute, University of Copenhagen, Lyngbyvej 2, Copenhagen DK-2100, Denmark
(5) Institute for Computational Cosmology, Physics Department, University of Durham, South Road, Durham DH1 3LE, UK

We study the stellar mass-gas-phase metallicity relation (MZR) as a function of the internal kinematics and morphology of galaxies in EAGLE cosmological simulations. According to our findings, at a given stellar mass (M_\star), gas-phase metallicity shows a clear secondary dependence on internal kinematics of galaxies and a more modest dependence on their morphologies. At the low-mass/high-mass end ($M_\star \leq 10^{10} M_\odot / M_\star \geq 10^{10} M_\odot$), systems with higher rotational support show lower/higher metallicities, on average. In addition, low-mass galaxies with more spheroidal stellar components tend to be more metal-enriched. More massive galaxies tend to exhibit flatter morphologies, with prolate systems being less metal-enriched, on average. As the redshift z increases, those aforementioned dependences of metallicity on kinematics and morphology tend to become weaker at low masses and stronger at high masses. These trends are consistent with the dependence of the MZR on gas fraction, star formation rate and stellar age, and the relation of the latter quantities with galaxy morpho-kinematics.

INTRODUCTION

The relation between stellar mass and gas-phase metallicity in galaxies (henceforth the mass-metallicity relation, MZR) has been studied extensively in the last decades from both an observational (Tremonti et al. 2004; Lara-López et al. 2010) and a theoretical (Calura et al. 2009; De Rossi et al. 2015; De Rossi et al. 2017; Sharma & Theuns 2019) point of view. Gas metallicity, Z , tends to increase with stellar mass, M_\star , approximately as a power law whose slope flattens towards higher masses. It is known that the scatter along the observed MZR correlates with other properties of galaxies (e.g., half-mass radius, star formation rate, gas fraction).

In this work, we examine the connection between the scatter around the MZR and internal morpho-kinematics of galaxies from the EAGLE cosmological hydrodynamical simulations. We found new predictions of EAGLE simulations regarding that connection, with trends that were not previously reported in MZR studies.

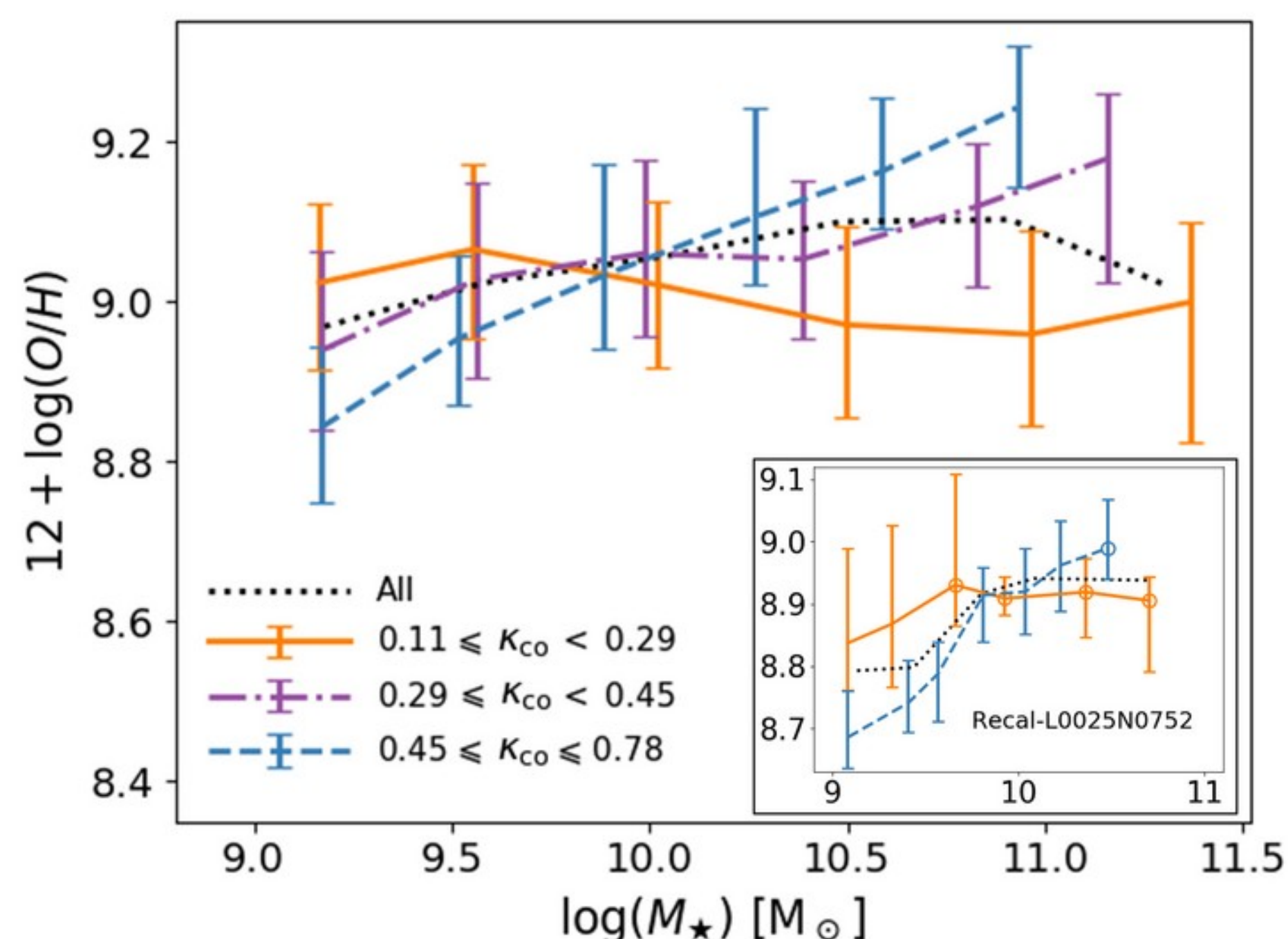
THE EAGLE SIMULATIONS

In this work, we use simulations of the EAGLE (Evolution and Assembly of GaLaxies and their Environments) suite of cosmological hydrodynamical simulations (Schaye et al., 2015). These simulations assume a standard Λ CDM cosmology, using the cosmological parameters of the Planck Collaboration (2015): $\Omega_\Lambda=0.693$, $\Omega_m=0.307$, $\Omega_b=0.048$ and $h=0.6777$.

We started working with the reference, intermediate-resolution simulation ('Ref-L0100N1504'), which has a co-moving extent of $L=100$ cMpc, with an initial baryonic particle mass of $1.2 \times 10^6 M_\odot$ (corresponding to 1504^3 particles) and a maximum proper softening length of 0.70 pkpc. We have verified that the main trends and conclusions presented in this work are consistent with those from the higher-resolution EAGLE simulation 'RecalL025N0752', analysed previously by De Rossi et al. (2017).

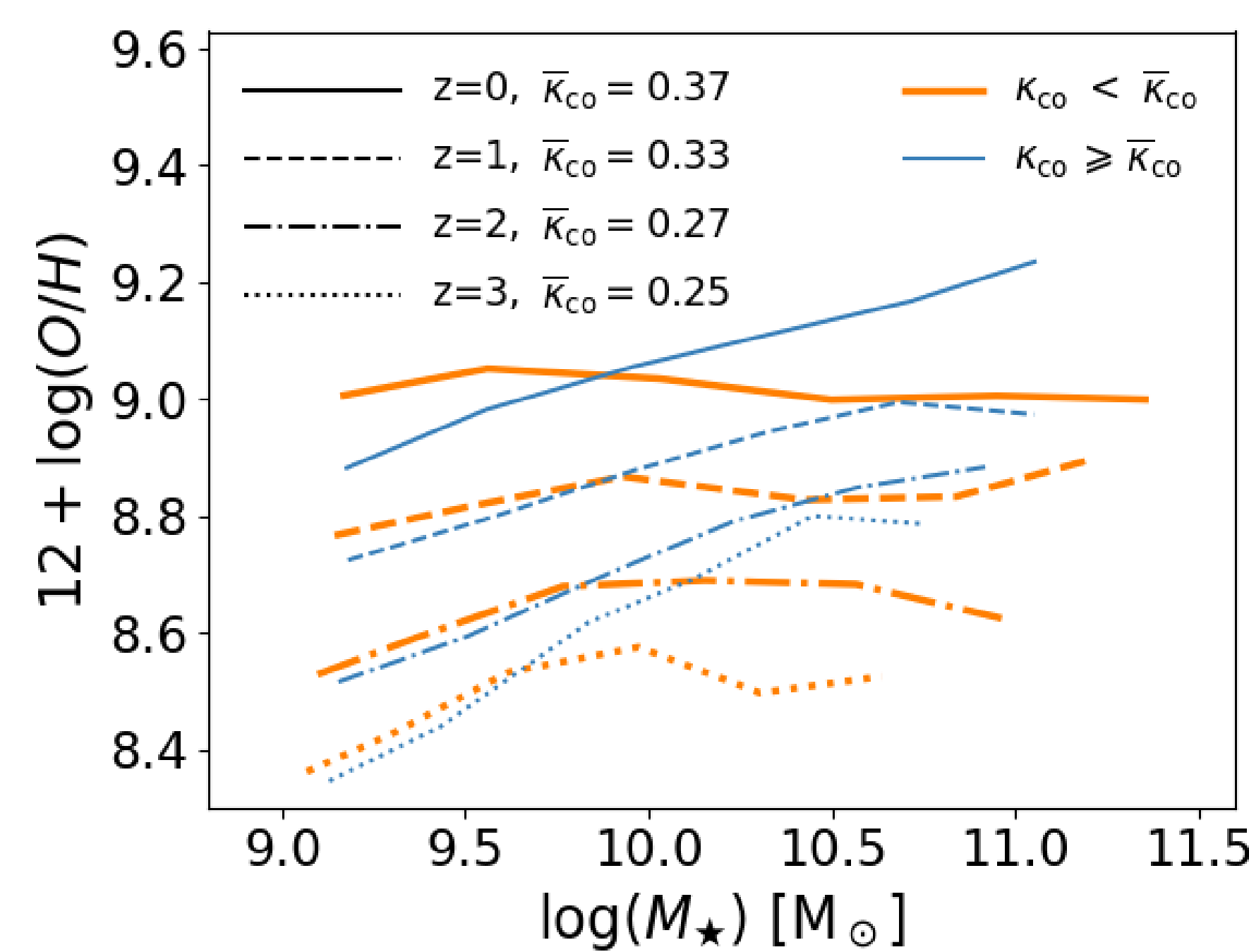
Both central and satellite galaxies were analysed in this work, measuring baryonic properties within spherical apertures of 30 pkpc. We use the O/H abundances of star-forming gas as an indicator of metallicity. We take into account only galaxies with at least 25 star-forming gas particles (gas mass of at least $5.25 \times 10^7 M_\odot$). Stellar morphology and kinematics are characterized by the fraction of kinetic energy in co-rotation (κ_{co}), the disc-to-total stellar mass ratio (D/T), the ratio of stellar rotation to velocity dispersion (V/σ), the ellipticity of the stellar body (ϵ_\star), and its triaxiality (T); all of these quantities are described in Thob et al. (2019).

MZR AS A FUNCTION OF STELLAR KINEMATICS



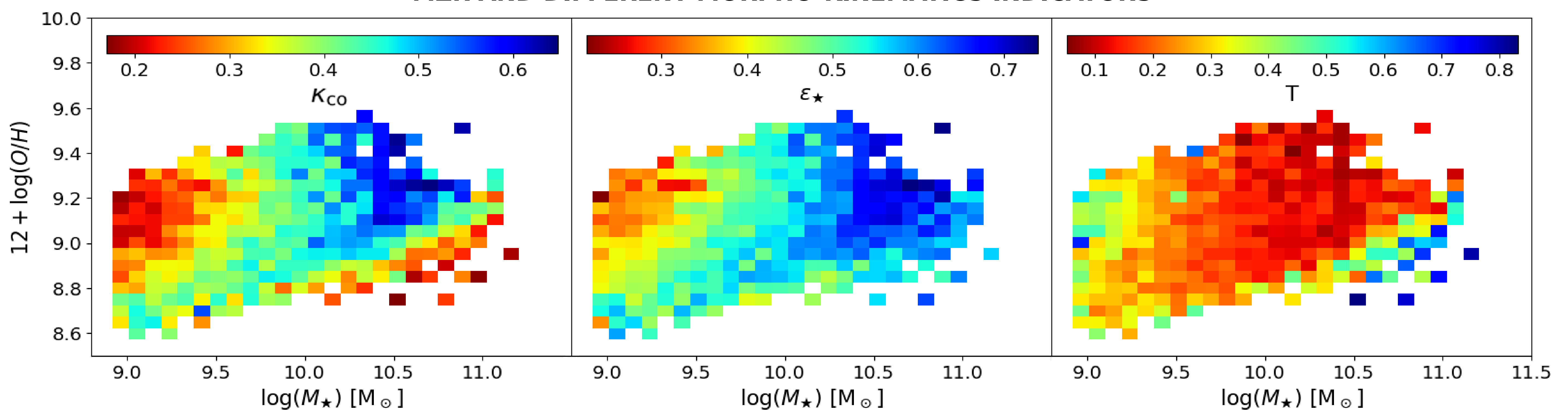
In the upper figure, the MZR at $z=0$ is shown, with galaxies binned by κ_{co} . Galaxies with stellar mass $M_\star \leq 10^{10} M_\odot$ that are dispersion-supported (low κ_{co} , orange line) have higher O/H than rotationally supported galaxies (blue line) of the same M_\star . Also, O/H increases with M_\star for rotationally supported galaxies, but is almost independent of M_\star for dispersion-supported galaxies. Therefore, the trend between O/H and κ_{co} inverts at $M_\star \geq 10^{10} M_\odot$, where dispersion-supported galaxies have lower O/H than rotationally supported ones of the same mass. Similar trends were found in the 'Recal-L025N0752' simulation (see inset figure).

MZR AND MORPHO-KINEMATICS AT DIFFERENT REDSHIFTS



The figure on the left shows the MZR relation at different redshifts z , being the sample of simulated galaxies separated in two sub-samples at a given z , using the median value of κ_{co} ($\bar{\kappa}_{co}$). As expected, the normalization of the MZR decreases with z . As at $z=0$, there is a clear increase of O/H with M_\star for galaxies with high κ_{co} , but this trend is mostly absent for low κ_{co} galaxies. As z increases, at $M_\star \leq 10^{10} M_\odot$ the secondary dependence of O/H on κ_{co} tends to vanish, while at $M_\star \geq 10^{10} M_\odot$ that dependence tends to be stronger. Similar evolutionary trends are obtained if using other morpho-kinematical indicators.

MZR AND DIFFERENT MORPHO-KINEMATICS INDICATORS



Upper panels show the O/H vs. M_\star plane at $z=0$ for our simulated sample of galaxies, with bins colour-coded according to the median values of κ_{co} (left), ϵ_\star (middle), and T (right). As can be seen, at $M_\star < 10^{10} M_\odot$, galaxies typically have low κ_{co} , but there is a tail of galaxies with high κ_{co} and low O/H. This tail generates an anti-correlation between κ_{co} and O/H, and as we checked, these galaxies are gas-rich; also, the middle and right panels show that these outliers have unusually high values of ϵ_\star and low values of triaxiality T. At $M_\star > 10^{10} M_\odot$, galaxies have usually a high value of κ_{co} , but now there is a tail of galaxies with low κ_{co} and high T that are typically more massive and have low O/H. At intermediate masses, $M_\star \sim 10^{10} M_\odot$, there is relatively little variation in κ_{co} or ϵ_\star .

SUMMARY AND WORK IN PROGRESS

- We analysed the stellar mass-gas metallicity relation (MZR) as function of morpho-kinematical parameters in the EAGLE cosmological hydrodynamical simulations.
- At $z = 0$, we found new secondary dependences of metallicity on the internal kinematics and morphology of simulated galaxies: at low masses ($M_\star < 10^{10} M_\odot$), higher metallicities are found for galaxies with more spheroidal morphologies and with lower rotational support. This trend inverts at high masses ($M_\star > 10^{10} M_\odot$).
- At higher redshifts, the secondary O/H dependence on morpho-kinematics becomes weaker for less massive galaxies, but stronger for more massive galaxies.
- These trends are consistent with secondary dependences of O/H (at a fixed mass) on gas fraction, star formation rate and stellar age studied by De Rossi et al. (2017).
- A detailed analysis of the origin and evolution of the Mass-Metallicity-Morphokinematics Relation in EAGLE is being carried out (Zenocratti et al., in prep.).

REFERENCES

- Calura F., Pipino A., Chiappini C., Matteucci F., Maiolino R., 2009, A&A, 504, 373
- Correa C. A., et al., 2017, MNRAS, 472, L45
- Crain R. A., et al., 2015, MNRAS, 450, 1937
- De Rossi M. E., Theuns T., Font A. S., McCarthy I. G., 2015, MNRAS, 452, 486
- De Rossi M. E., Bower R. G., Font A. S., Schaye J., Theuns T., 2017, MNRAS, 472, 3354
- Lara-López M. A., et al., 2010, A&A, 521, L53
- Mannucci F., Cresci G., Maiolino R., Marconi A., Gnerucci A., 2010, MNRAS, 408, 2115
- Planck Collaboration, et al., 2015, A&A, 580, A22
- Schaye J., et al., 2015, MNRAS, 446, 521
- Sharma M., Theuns T., 2020, MNRAS, 492, 2418
- The EAGLE team 2017, ArXiv e-prints: 1706.09899
- Thob A. C. R., et al., 2019, MNRAS, 485, 972
- Tremonti C. A., et al., 2004, ApJ, 613, 898
- Zenocratti L. J., et al., 2020, ArXiv e-prints: 1911.09571

FOR MORE DETAILS ABOUT THIS WORK, SEE ZENOCRATTI ET AL. (2020)